

J. M. Nóbrega<sup>1</sup>, O. S. Carneiro<sup>1\*</sup>, P. J. Oliveira<sup>2</sup>, F. T. Pinho<sup>3</sup>

<sup>1</sup>Department of Polymer Engineering, Universidade do Minho, Guimarães, Portugal

<sup>2</sup>Departamento de Engenharia Electromecânica, Universidade da Beira Interior, Covilhã, Portugal

<sup>3</sup>Centro de Estudos de Fenómenos de Transporte, DEMEGI, Faculdade de Engenharia da Universidade do Porto, Porto, Portugal

# Flow Balancing in Extrusion Dies for Thermoplastic Profiles

## Part I: Automatic Design

*To achieve a specified geometry for an extruded profile, together with a minimal degree of internal stresses, flow balancing of the die is required. To attain this objective, the flow along a profile die channel must be accurately described, and this demands a computational code able to predict complex 3D non-isothermal flow patterns. In this work new methodologies for flow balancing are implemented and illustrated. The design code developed to carry out the automatic search of a final geometry consists of an optimisation routine coupled with geometry and mesh generators and a 3D computational code based on the finite volume method. The issues discussed and described here encompass recent developments, namely the implementation of two alternative optimisation algorithms for the automatic search of a final solution, the enhancement of the strategies previously developed to balance the flow, some improvements in the routine used to generate the mesh and the adoption of a progressive mesh refinement technique. The examples show that the proposed methodology performs well and the solution is attained in just a few minutes of calculation without any user intervention during the calculation process.*

### 1 Introduction

In the past, the design of profile extrusion dies was based on experimental trial-and-error procedures, relying essentially on the designers experience and usually being very time, material and equipment consuming [1, 2]. Currently, due to the development of software packages for the mathematical modelling of the flow of polymer melts [3 to 7] this trial-and-error procedure is being progressively transformed from an experimental to a numerical based operation. However, the generation of the successive solutions, and the decisions necessarily involved in this process, are still committed to the designer [1].

To achieve the specified geometry for an extruded profile, together with a minimal degree of internal stresses, flow balancing of the die is required. These requisites depend essentially of the geometry of the flow channel and of the rheological properties of the polymer melt and their dependence on both shear rate

and temperature. Therefore, the flow along a profile die channel must be accurately described, demanding a computational code able to predict the complex 3D flow patterns involved and the corresponding local fluid temperature variations promoted by viscous heat dissipation [8] and/or specific thermal boundary conditions, especially in the case of thin complex cross-section geometries encompassing different local flow restrictions. Therefore, flow balancing has a major relevance, being one of the steps of a broader global design methodology for profile extrusion dies that has been developed by the authors [9 to 11].

This work is a contribution towards the *automatic extrusion die design concept* and it focuses on improvements implemented both in an existing computational code based on the finite volume method [12] and in a profile extrusion die design methodology [9]. The main improvements described here are:

- i) the implementation of two alternative optimisation algorithms to enable the automatic search of a final solution;
- ii) enhancements on the methodology adopted to attain the flow balancing, including the possibility of varying not only the length but also the thickness of the die parallel zone;
- iii) improvements of the efficiency and accuracy of the numerical simulations through the use of local computational grid refinements at locations where severe gradients of the flow field are expected to occur;
- iv) the adoption of a progressive mesh refinement technique to reduce the computation time required for calculations;
- v) the introduction of the energy equation, accounting for viscous dissipation and temperature dependent viscosity, in order to enable the characterisation of more realistic non-isothermal flows.

The first part of this work (section 2) focuses essentially on the contribution towards the *automatic extrusion die design concept* and describes the methodology developed to automatically balance the flow. Section 3 describes the scheme implemented to carry out the automatic search of the final solution and the integration of the different routines required, namely the pre-processor, the computational rheology code and the optimisation algorithm. Section 4 deals with the computational rheology code, and in particular describes the modifications demanded by the inclusion of the energy equation. The methodology is applied to a particular case study presented in section 5. Results are discussed in section 6 and finally conclusions of the work are drawn in section 7.

\* Mail address: O. Carneiro, Department of Polymer Engineering, Universidade do Minho, 4800-058 Guimarães, Portugal

## 2 Methodology

For design purposes, the extrusion die flow channel is divided into four particular geometrical zones, namely, the die land or parallel zone (PZ), the preparallel zone (PPZ), the transition zone (TZ) and the adapter (A), as illustrated in Fig. 1. However, since the flow distribution is dominated by the most restrictive zones, PZ and PPZ [1, 2, 9], and the flow occurring in upstream regions, TZ and A, has negligible contribution to viscous heating, for flow balancing purposes it will be sufficient to model the flow in the (PPZ + PZ) domain. The PZ and PPZ cross sections are divided into elemental sections (ES) [9], each being defined by adjustable geometrical parameters that enable the control of the local flow restriction, and regions corresponding to the intersections (I) of several ES, shown in Fig. 2. The controllable geometrical parameters of the PPZ and PZ are those shown in Fig. 1: distance to the die exit, or length of constant thickness, (L), angle of convergence ( $\theta$ ) and

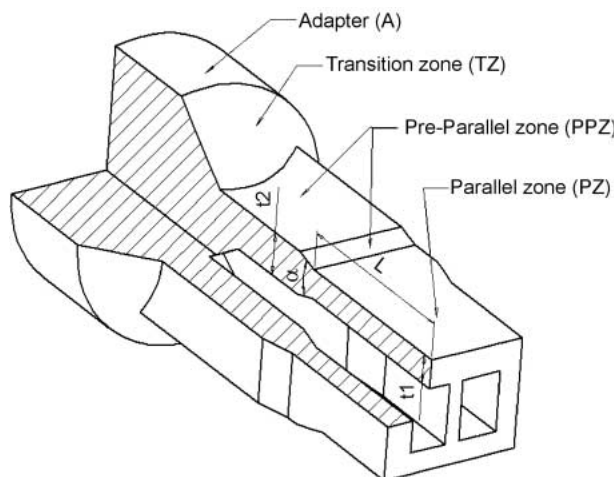


Fig. 1. Flow channel of a profile extrusion die: identification of its main zones and geometrical controllable parameters considered in the definition of the PPZ

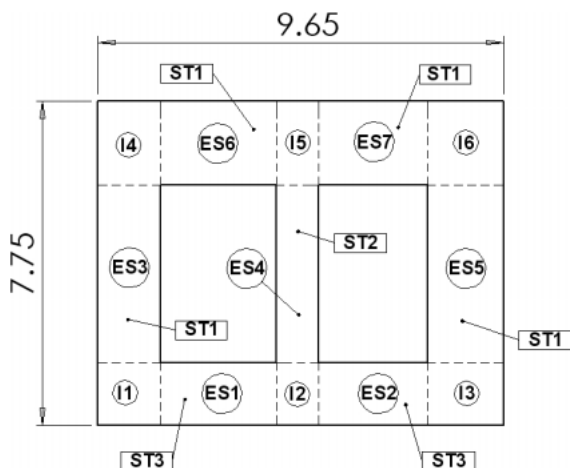


Fig. 2. Cross section of the parallel zone (PZ) of the profile die used as a case study (dimensions in mm): subdivision in elemental (ES) and intersection (I) sections and identification of the strategy (ST) adopted to optimise each ES

compression ratio ( $t_2/t_1$ ) [9 to 11]. The next step of the automatic design procedure consists in the selection of the flow balance strategy adopted to balance the flow in each ES. There are three possible strategies in this method:

- i) find the best ES length in order to obtain a local average velocity equal to the global average flow velocity [2, 8 to 11]. In this strategy (Strategy ST1) the ES thickness is equal to that of the profile;
- ii) find the best ES thickness in order to obtain a local ES flow rate that allows the attainment of the pre-established thickness after pulling [2, 8] (Strategy ST2);
- iii) find the best ES thickness in order to obtain a local average velocity equal to the global average flow velocity (Strategy ST3). As is discussed in a forthcoming paper [13], this strategy combines the advantages of the previous but has a drawback, since the section thickness cannot be imposed.

In all cases the remaining controllable parameters are kept unchanged.

The methodology proposed in this work combines the referred strategies (ST1, ST2 and ST3) and its application is expected to result in a final die channel geometry that minimises the stress gradient induced by pulling on the extruded profile while exhibiting a performance less dependent on the operating conditions. To complement this work, a study of the performance and sensitivity of dies optimised by means of the design strategies mentioned above is left to a forthcoming paper [13].

## 3 Optimisation Process

The aim of the optimisation methodology here developed is to automatically find the set of geometrical parameters that results in the most balanced geometry. Fig. 3 illustrates schematically the integration of the different routines needed for this

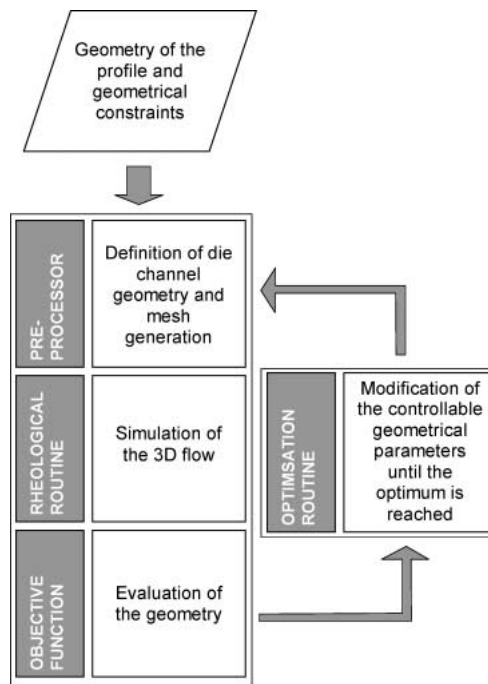


Fig. 3. Optimisation methodology flow chart

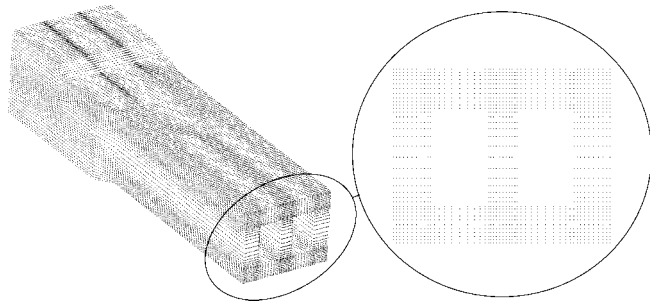


Fig. 4. Typical mesh used in the calculations

purpose. The process begins with the definition of a trial geometry for the flow channel and the imposition of the geometrical constraints. Here, for each ES, the maximum and minimum admissible values for the ratio length/thickness ( $L/t$ ) are considered to be 15 and 1, respectively, regardless of the profile to be extruded. However, a penalty function will be applied to  $L/t$  values below 7, as because lower values for this ratio are not recommended [14]. Furthermore, to guarantee a final realistic solution for the extrusion die, conditions of equality of thickness or length may be imposed to different elemental sections, whenever these are supposed to be machined in a single step. So, this type of restriction is dependent of the particular profile being designed.

During the optimisation process a pre-processor is used to generate automatically the computational grid corresponding to each geometry proposed by the optimisation algorithm. In order to improve the efficiency and/or accuracy of the numerical simulations, the pre-processor generates smooth grids, with cellsize continuity, and refines the mesh along the flow channel thickness (relative to the length and width dimensions), particularly near the walls, where severe gradients of the flow quantities are expected to occur (see Fig. 4).

In order to reduce the time required for the computation, the calculation starts with coarse meshes and progressively performs mesh refinements as the optimisation algorithm evolves towards a final solution.

After having carrying out the corresponding 3D non-isothermal flow simulation, the quality of each trial geometry is assessed by an objective function ( $F_{obj}$ ), which combines two criteria – flow balance and ratio  $L/t$  – affected by different weights, each term being weighted by the cross section area of the respective region, as in Eq. 1:

$$F_{obj} = \sum_{i=1}^{n_z} \left\{ \left\{ \psi \left( 1 - \frac{V_i}{V_{obj,i}} \right)^2 + k(1 - \psi) \left[ 1 - \frac{(L/t)_i}{(L/t)_{min}} \right]^2 \right\} \frac{A_{obj,i}}{A_{obj}} \right\} \quad (1)$$

where:  $n_z$ : total number of ES and I zones considered;  $k$ : 0 for all I zones and for ES zones with  $(L/t)_i \geq (L/t)_{min}$ ;  $k$ : 1 for ES zones with  $(L/t)_i < (L/t)_{min}$ ;  $V_i$ : actual average velocity of the melt flow in each zone;  $(L/t)_i$ : ratio between the length and thickness of each ES;  $(L/t)_{min}$ : minimum value recommended for the ratio  $L/t$  (here considered to be 7);  $\psi$ : relative weight;  $A_{obj}$ ,  $A_{obj,i}$ : objective cross section areas of the global flow channel and of each zone, respectively;  $A_i$ : actual cross

section area of each zone;  $\bar{V}$ : global flow average velocity;  $V_{obj,i}$ : objective average velocity of the melt flow in each zone, given by the continuity equation:

$$V_{obj,i} = \bar{V} \frac{A_{obj,i}}{A_i} \quad (2)$$

The objective function is defined in such a way that its value decreases with increasing performance of the die, being zero for a perfectly balanced condition with all the ES lengths in the advisable range. In this work  $\psi$  has taken the value of 0.75, in order to emphasize the importance of flow balance rather than that of the ratio  $L/t$ .

Two optimisation algorithms were implemented. One is based on the non-linear SIMPLEX method (SM) [15] and the other tries to mimic the conventional trial-and-error experimental procedure used in the manufacture of a new extrusion die (EM), i. e. the geometry changes are carried out in order to facilitate the flow in sections where the melt flow rate is lower than the required value, and vice-versa. These algorithms were implemented in computer routines that adjust the PPZ controllable geometrical parameters until an optimum design is reached, according to the sequences defined in Figs. 5 and 6.

The SIMPLEX method (see Fig. 5) starts with 'n + 1' trial geometries randomly generated, with n being the number of optimisation variables considered. After the corresponding simulations of the flow, the worst solution (in terms of objective function value) is rejected and is replaced by a new trial geometry proposed by the SIMPLEX method (see Fig. 5). When the standard deviation of the objective function, corresponding to the 'n + 1' trial solutions, is smaller than a prescribed value the mesh is refined. Under the conditions described above, the calculation finishes when the highest mesh refinement stage is achieved. More details about the SIMPLEX method can be found in [15].

The *experimental method* (see Fig. 6) starts with a trial solution defined by the user. After evaluation and calculation of the correction factors (CF), defined as the ratio between the actual and the desired flow rate corresponding to the region controlled by each variable, the algorithm tries to improve the solution using the following operations in sequence:

- i) correct all the optimisation variables using the calculated CF;
- ii) return to the previous solution and correct the optimisation variable of the region that has the worst contribution to the objective function value by  $0.5 \cdot CF$ ;
- iii) return to the previous solution, correct the optimisation variable of the region that most contributed to the improvement of the objective function value by  $0.5 \cdot CF$ .

If none of the previous operations is able to improve the objective function value the mesh is refined. The calculation ends when the highest mesh refinement stage, defined by the user, is achieved.

#### 4 Outline of the Numerical Procedure (Rheological Routine)

The calculation of the flow field is performed by a self-contained part of the code that has been developed for the computation of isothermal viscoelastic flows, recently extended to

deal with non-isothermal flows [16], which is described and tested in detail in a series of papers [12, 17]. In this section, a quick overview of the calculation procedure is given. The basic equations to be solved are those expressing conservation of mass, linear momentum and energy,

$$\frac{\partial \rho u_j}{\partial x_j} = 0, \tag{3}$$

$$\frac{\partial \rho u_i}{\partial t} + \frac{\partial \rho u_j u_i}{\partial x_j} = -\frac{\partial p}{\partial x_i} + \frac{\partial \tau_{ij}}{\partial x_j}, \tag{4}$$

$$\frac{\partial \rho c T}{\partial t} + \frac{\partial \rho c u_i T}{\partial x_i} = \frac{\partial}{\partial x_i} \left( k \frac{\partial T}{\partial x_i} \right) + \tau_{ij} \frac{\partial u_i}{\partial x_j} \tag{5}$$

and a constitutive rheological equation for the stress field  $\tau_{ij}$ . In these equations  $u_i$  is the velocity component in a Cartesian co-

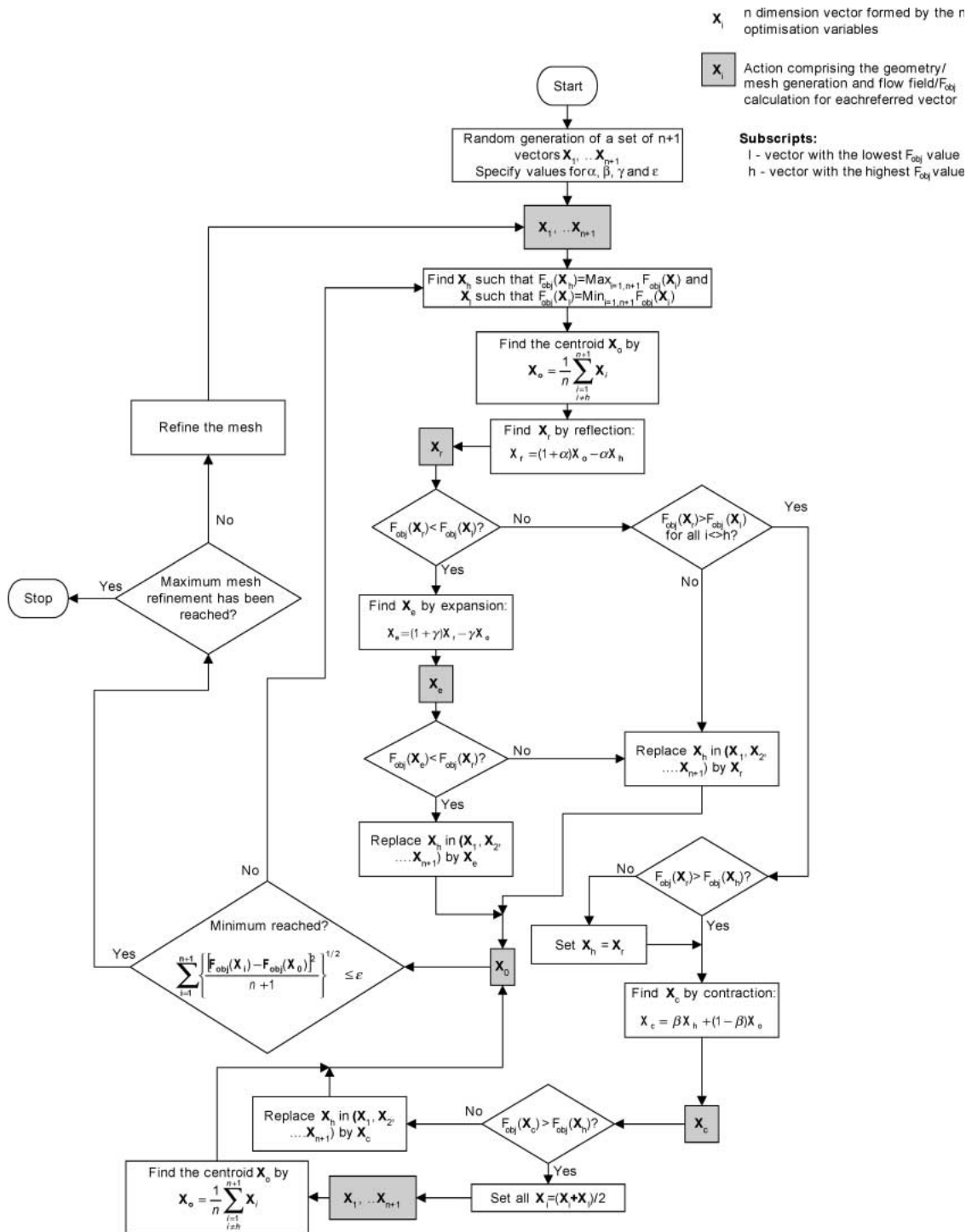


Fig. 5. Optimisation sequence corresponding to the SIMPLEX method (SM)

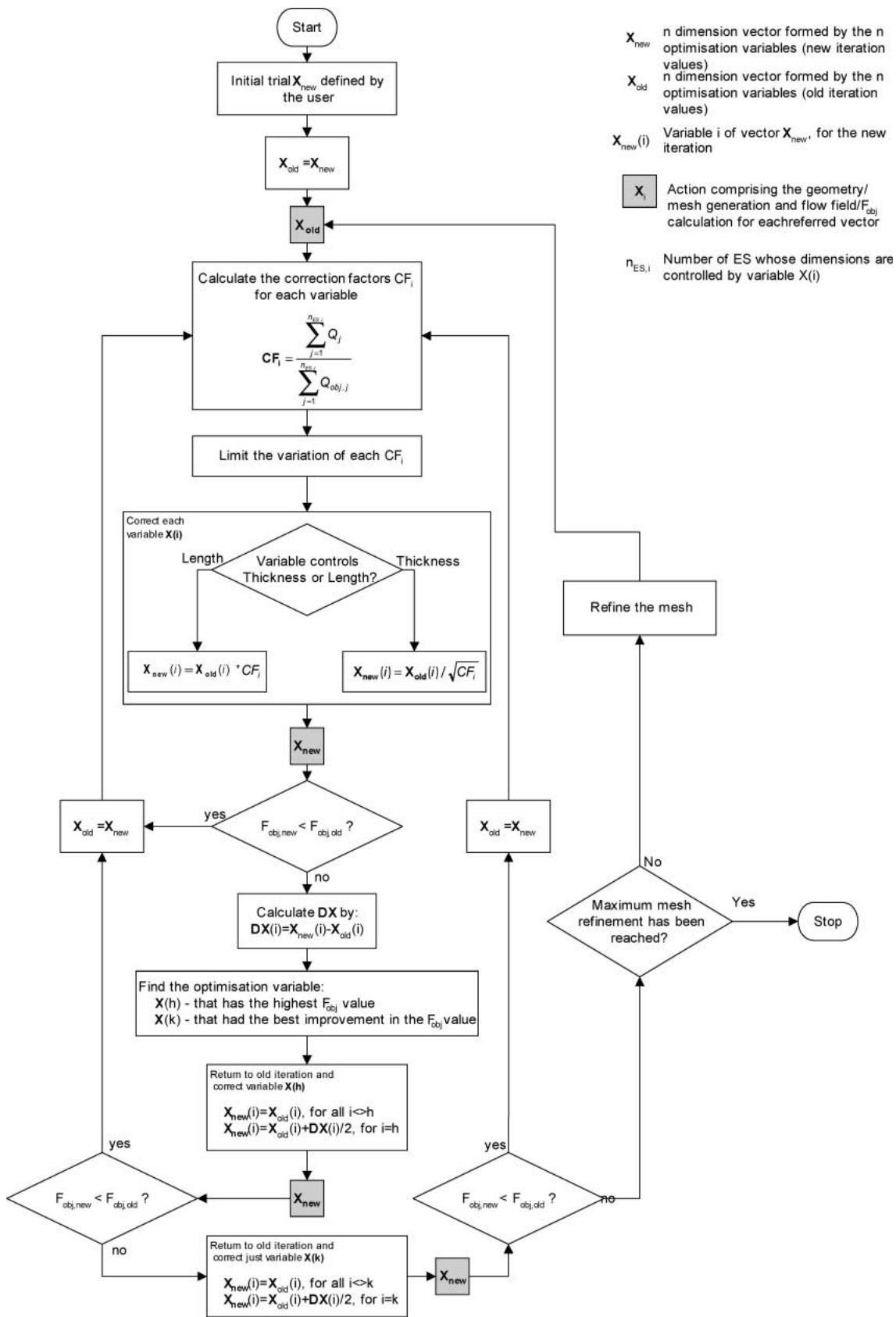


Fig. 6. Optimisation sequence corresponding to the experimental method (EM)

ordinate frame,  $\rho$  is the fluid density,  $p$  is an isotropic pressure,  $T$  is the temperature,  $k$  is the thermal conductivity and  $c$  is the specific heat. The last term on the righthandside of Eq. 5 accounts for the viscous dissipation. Although the interest is on steady flows, the time dependent term in Eqs. 4 and 5 are retained because the solution is reached following a time marching approach. In the present computations the generalised Newtonian fluid rheological constitutive equation was considered

$$\tau_{ij} = \eta(\dot{\gamma}, T) \left( \frac{\partial u_i}{\partial x_j} + \frac{\partial u_j}{\partial x_i} \right) - \frac{2}{3} \eta(\dot{\gamma}, T) \frac{\partial u_k}{\partial x_k} \delta_{ij}, \quad (6)$$

where  $\eta$  is the dynamic viscosity of the fluid. The velocity divergence in the last term of Eq. 6 vanishes for incompressible flows, but is kept in the code for stability reasons. The dynamic viscosity is a function of temperature and of the second invariant of the rate of deformation tensor  $\dot{\gamma} \equiv \sqrt{2\text{tr}\mathbf{D}^2}$  where

$$D_{ij} = \frac{1}{2} \left( \frac{\partial u_i}{\partial x_j} + \frac{\partial u_j}{\partial x_i} \right) \quad (7)$$

In this paper, the adopted viscosity model was  $\eta(\dot{\gamma}, T) = F(\dot{\gamma})H(T)H(T)$ . The shear rate dependence contribution was here assumed to follow a Bird-Carreau equation [18]:

$$F(\dot{\gamma}) = \eta_\infty + \frac{\eta_0 - \eta_\infty}{\left(1 + (\lambda\dot{\gamma})^2\right)^{\frac{1-n}{2}}}, \quad (8)$$

where  $\eta_\infty$  is the infinite-shear-rate viscosity,  $\eta_0$  is the zero-shear-rate viscosity,  $\lambda$  is a time constant (i.e., the inverse of the shear-rate at which the fluid changes from Newtonian to power-law behaviour) and  $n$  is the power-law index. The Arrhenius law was used to account for the viscosity temperature dependence:

$$H(T) = \exp \left[ \frac{E}{R} \left( \frac{1}{T} - \frac{1}{T_{\text{ref}}} \right) \right], \quad (9)$$

where  $E$  is the activation energy,  $R$  the universal gas constant and  $T_{\text{ref}}$  is the reference temperature (in Kelvin) for which  $H(T) = 1$ .

Given the similarity between the energy (Eq. 5) and linear momentum (Eq. 4) equations, the discretisation and numerical solution of the former is equivalent to that of the linear momentum provided  $u_i$  is substituted by  $T$  and the coefficients of the equations are modified in accordance with the original conservation equations [16]. The numerical solution of the energy equation was inserted into the sequential algorithm, being the last equation of the set to be solved at each time step, with convection fluxes and dissipation terms based on the previously calculated velocity field.

## 5 Case Study

The polymer used in the simulations was a polypropylene homopolymer extrusion grade, Novolen PPH 2150, from Targor. Its rheological behaviour was experimentally characterised in capillary and rotational rheometers, at 210 °C, 230 °C and 250 °C. The shear viscosity data was fitted with least-squares method by means of the Bird-Carreau constitutive equation combined with the Arrhenius law given above

(Eqs. 8 and 9), considering  $T_{\text{ref}} = 230$  °C and  $\eta_\infty = 0$  Pa · s, yielding the following parameters:  $\eta_0 = 5.58 \times 10^4$  Pa · s,  $\lambda = 3.21$ ,  $n = 0.3014$ ,  $E/R$  (°C) =  $2.9 \times 10^3$ .

The proposed flow balancing methodology described in sections 2 and 3 was used to improve the design of the flow channel of the extrusion die shown in Fig. 1, by adopting the division in elemental sections (ES) illustrated in Fig. 2. In this example, strategy ST3 was selected for ES1 and ES2, as they are both supposed to be part of a profile wall without pre-defined thickness. It was also considered that ES3, ES5, ES6 and ES7 must have pre-defined thickness and high dimensional stability in use; therefore, ST1 was selected for these sections. Finally, it was assumed that the inner wall of the profile must have a pre-defined thickness to avoid differential cooling in the calibrator, but its dimensional stability is less important; in this case, strategy ST2 was selected. The optimisation strategies adopted for each ES are summarized in Fig. 2, for easy reference.

Different wall thicknesses were intentionally considered for the profile (see Fig. 2), in order to enforce an imbalanced geometry. The initial/reference dimensions considered for the die flow channel are shown in Table 1. The remaining dimensions of the PPZ, defined in Fig. 1, were fixed for all the ES: entrance thickness ( $t_2$ ) of 3 mm and convergence angle ( $\theta$ ) of 30°.

ES	1	2	3	4	5	6	7
$t_i$ [mm]	1.5	1.5	1.5	1.0	1.8	2.0	2.0
$L_i$ [mm]	22.5	22.5	22.5	15.0	27.0	30.0	30.0

Table 1. Initial flow channel dimensions

The geometry was optimised using both the *experimental method* (EM) and the *SIMPLEX method* (SM). For both cases the following 5 controllable variables were considered:

- Opt1 – for ES1 and ES2 thickness;
- Opt2 – for ES3 length;
- Opt3 – for ES4 thickness;
- Opt4 – for ES5 length;
- Opt5 – for ES6 and ES7 length.

Due to machining requirements ES1 and ES2 thickness and ES6 and ES7 length were considered to be equal. For the SM method the values adopted for the parameters  $\alpha$  (reflection),  $\beta$  (contraction),  $\gamma$  (expansion) and  $\varepsilon$  (accuracy factor), defined in Fig. 5, were of 1.0, 0.5, 2.0 and 0.001, respectively. For the EM method, the maximum variation allowed for the correction factors, CF (defined in Fig. 6), was set to 20 %.

The operating and thermal boundary conditions used in the flow simulations are defined in Table 2.

Flow rate*	16.7 kg/h
Melt inlet temperature	230 °C
Outer die walls temperature	230 °C
Inner (mandrel) die walls	Adiabatic

\* Corresponding to an average velocity of 100 mm/s at the die exit

Table 2. Operating and thermal boundary conditions used in the flow simulations

As mentioned before, in the first iterations the computational grid was rather coarse, being each ES mapped with only 2 cells along the thickness. A typical grid used at the final stages of the calculations, with 10 cells along the thickness (corresponding to a total of 160 000 cells for the whole geometry), is shown in Fig. 4. For this refined mesh, the typical calculation time required in each iteration (including the time needed for the mesh generation and the flow field calculation) was about 1.25 h using a Pentium III computer running at 933 MHz, whereas each of the initial iterations took around 30 s.

### 6 Results and Discussion

The results obtained along the iterative process for optimisation of the flow distribution are illustrated here in terms of the variations of the objective function, the ratio  $V/V_{obj}$  and the ratio  $Opt/Opt_{ref}$  in Figs. 7 and 8, for the *experimental* (EM) and the SIMPLEX (SM) methods, respectively. In these ratios the  $Opt_{ref}$  values are defined by the corresponding initial values of these variables and the objective average velocity  $V_{obj}$  is calculated using Eq. 2.

A positive conclusion drawn from Figs. 7 and 8 is that the final solutions, obtained from the application of both optimisation algorithms, are similar in terms of objective function and final value of almost all variables, the only noteworthy exception being the value obtained for Opt4 (length of ES5), as quantified in Table 3. This suggests that the global flow distribution is almost insensitive to Opt4 variable. Another important conclusion is that the EM methodology should be preferred, since it requires less iterations than the SM (as shown in Figs. 7 and 8) and, consequently, it has smaller calculation time, being about 1/3 of that corresponding to SM (see Table 4, where the relative differences and the computing times of the two methods are compared).

	Optimisation variable ( $Opt_i$ )				
	1	2	3	4	5
Initial (reference)	1.50	22.5	1.00	27.0	30.0
Final (EM)	1.87	9.0	1.25	24.6	30.0
Final (SM)	1.92	6.0	1.23	9.5	24.0

Table 3. Initial (reference) and final values of the variables used in the optimisation procedure (dimensions in mm)

		Number of cells along thickness					Total
		2	4	6	8	10	
Maximum difference to final solution	EM	0 %	0 %	0 %	0 %	0 %	
	SM	15 %	15 %	17 %	2 %	0 %	
Calculation time [h : m]	EM	0 : 06	0 : 10	0 : 53	2 : 39	5 : 03	8 : 53
	SM	0 : 32	0 : 23	3 : 48	8 : 37	16 : 45	24 : 45

Table 4. Evolution of the maximum difference experienced by the optimisation variables and computational time corresponding to each mesh refinement stage

As expected from the initial profile geometrical imbalance, there are significant differences in the average ES velocities at the first iteration and, consequently, the objective function takes on a high value. After optimisation, a reasonable improvement is obtained with a fourfold decrease in the  $F_{obj}$ . Nevertheless, in the final solution the average melt velocity in

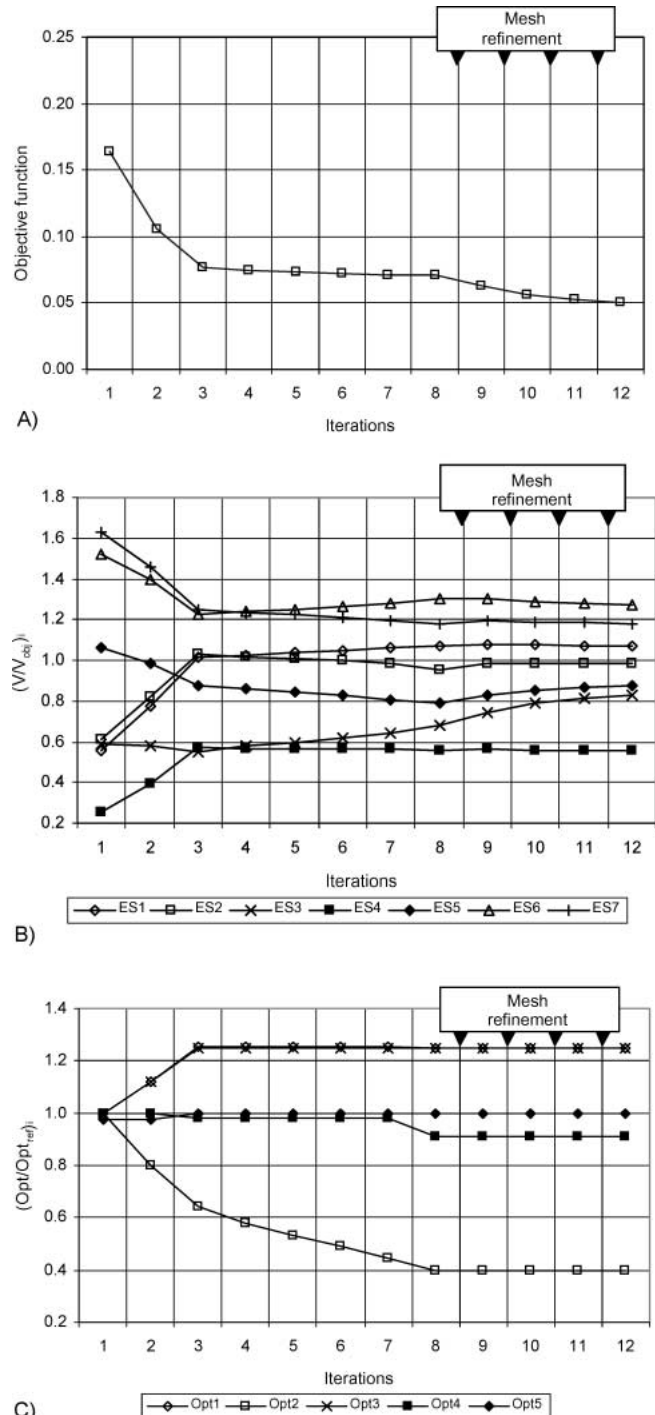


Fig. 7. Results of simulations performed during the optimisation process for the experimental method (EM): (A) objective function; (B) relative average velocity in each elemental section; (C) ratio between the actual value of the optimisation variable and the corresponding reference value

ES4, the thinnest section, is almost 50 % away from the global bulk velocity. This effect is a consequence of the pronounced geometrical imbalance imposed to this profile, which is expected to be minimised by the consideration of alternative design methodologies [13].

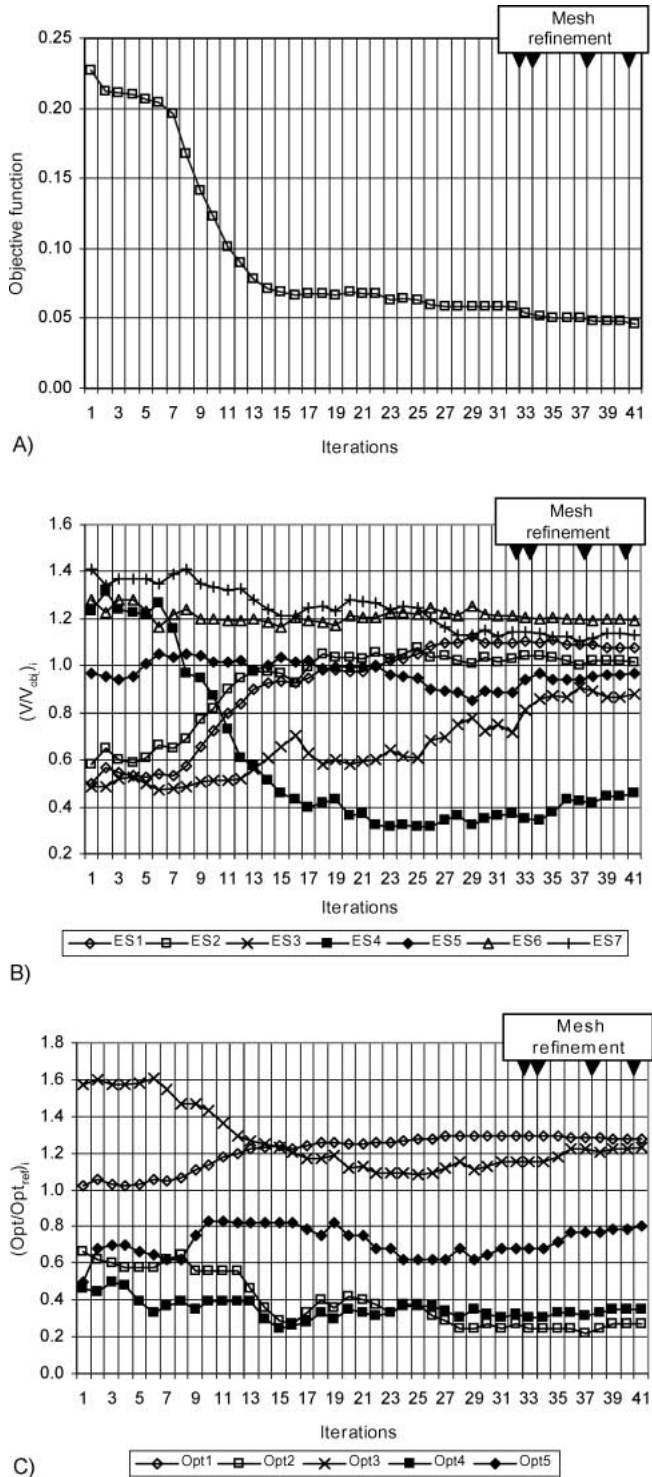


Fig. 8. Results of simulations performed during the optimisation process for the SIMPLEX method (SM): (A) objective function; (B) relative average velocity in each elemental section; (C) ratio between the actual value of the optimisation variable and the corresponding reference value

Table 4 shows the evolution of the maximum difference experienced by the controllable variables, computed using their values at the end of each mesh refinement stage and those corresponding to the final solution obtained; the computational time corresponding to all iterations performed in each stage is also shown. In Figs. 7 and 8 black arrows mark the iterations where mesh refinements occurred (in the sequence 2, 4, 6, 8, 10). These results indicate that even the meshes with 2 cells along the thickness were able to predict quite accurately the flow distribution (in fact the EM algorithm reached the final solution at this stage). Therefore, the subsequent mesh refinements were only useful for assessment purposes. However, it is worth mentioning that the use of the more refined meshes may be essential if accurate absolute values for the velocity, pressure and temperature fields are required. In fact, since at

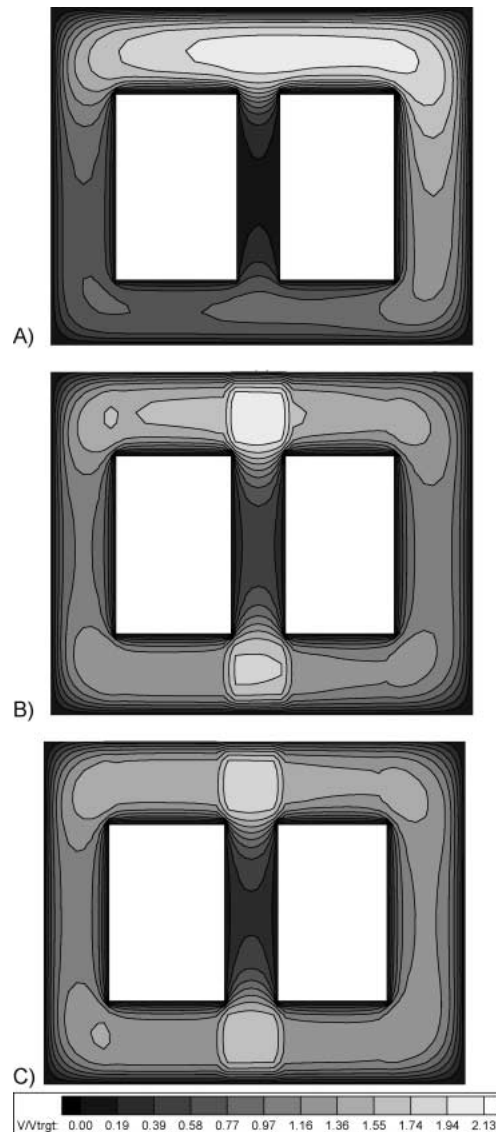


Fig. 9. Contours of the ratio between the axial velocity and the objective velocity computed for: (A) initial trial geometry; (B) best result obtained by the experimental methodology and (C) best result obtained by the SIMPLEX methodology

the beginning of each mesh refinement stage the trial geometry is maintained, i. e., it is equal to the best obtained in the previous step, the minor variations occurring for the  $F_{obj}$  value (see Figs. 7 and 8) were just motivated by the improved calculation accuracy. Despite the total number of hours required to finish the calculations using the EM algorithm (about eight hours with the computer here employed), it is interesting to point out that for this case study the final solution is achieved in just 6 min.

The improvement obtained for the velocity field may be assessed through comparison of the contours of relative velocity shown in Fig. 9. Clearly, the velocity distribution is much flatter after application of the automatic flow balance methodology, hence yielding a better flow distribution.

## 7 Conclusion

The automatic die design methodology used in this work has shown great potential since it performs well and quickly in designing a complex profile geometry without any user intervention during the optimisation procedure.

The methodology includes a three-dimensional flow solver developed for the numerical simulation of the non-isothermal polymer melt flow. When coupled with the progressive mesh-refinement technique here suggested, it resulted in a reasonable solution to the flow balance problem in just a few minutes of calculation.

The two optimisation algorithms that have been developed, implemented and tested lead to similar final die geometries with similar performances, a reassuring result, but the algorithm based on the *experimental methodology* proved to be swifter than that based on the non-linear SIMPLEX method, requiring circa 1/4 of the total number of iterations and 1/3 of the total computational time.

## References

- 1 Szarvasy, I., Sienz, J., Pitman, J. F. T., Hinton, E.: Int. Polym. Process. 15, p. 28 (2000)
- 2 Sienz, J., Bulman, S. D., Pitman, J. F. T.: Paper presented at the 4<sup>th</sup> ESAFORM Conference, Liege, Belgium, April (2001)
- 3 Software Polyflow, Fluent Inc.
- 4 Software Flow 2000, Compuplast.
- 5 Menges, G., Kalwa, M., Schmidt, J.: Kunststoffe 77 (8), p. 797 (1987)
- 6 Vlachopoulos, J., Behncke, P., Vlcek, J.: Adv. Polym. Tech. 9 (2), p. 147 (1989)
- 7 Sebastian, D. H., Rakos, R.: Adv. Polym. Tech. 5, p. 333 (1985)
- 8 Svabik, J., Placek, L., Saha, P.: Int. Polym. Process. 14, p. 247 (1999)
- 9 Carneiro, O. S., Nóbrega, J. M., Pinho, F. T., Oliveira, P. J.: J. Mat. Process. Tech. 114, p. 75 (2001)
- 10 Nóbrega, J. M., Carneiro, O. S., Pinho, F. T., Oliveira, P. J.: Paper presented at the SPE Annual Technical Conference, Dallas, USA, May (2001)
- 11 Nóbrega, J. M., Carneiro, O. S., Pinho, F. T., Oliveira, P. J.: Paper presented at the 17<sup>th</sup> Annual Meeting of the Polymer Processing Society, Montreal, Canada, June (2001)
- 12 Oliveira, P. J., Pinho, F. T., Pinto, G. A.: J. Non-Newt. Fluid Mech. 79, p. 1 (1998)
- 13 Carneiro, O. S., Nóbrega, J. M., Pinho, F. T., Oliveira, P. J.: Int. Polym. Process. 18, p. ■ (2002)
- 14 Michaeli, W.: Extrusion Dies for Plastic and Rubber. Hanser Publishers, Munich, Vienna, New York (1992)
- 15 Rao, S. S.: Optimization Theory and Applications. Wiley Eastern Limited (1984)
- 16 Nóbrega, J. M., Pinho, F. T., Oliveira, P. J., Carneiro, O. S.: Characteristics of laminar duct flows for viscoelastic fluids with temperature dependent properties. Preliminary version of Internal report of Department of Polymer Engineering, University of Minho, 2002.
- 17 Oliveira, P. J., Pinho, F. T.: Num. Heat Transfer, Part B 35 (3), p. 295 (1999)
- 18 Baird, D. G., Collias, D. I.: Polymer Processing – Principles and Design. Butterworth-Heinemann (1995)

*Date received: July 26, 2002*

*Date accepted: March 4, 2003*